Supplement of Earth Syst. Sci. Data, 15, 2601–2622, 2023
https://doi.org/10.5194/essd-15-2601-2023-supplement

Supplement of

A gridded dataset of a leaf-age-dependent leaf area index seasonality product over tropical and subtropical evergreen broadleaved forests

Xueqin Yang et al.

Correspondence to: Xiuzhi Chen (chenxzh73@mail.sysu.edu.cn)

Supplementary Methods

(1) ERA-Interim VPD

We calculated vapor pressure deficits (VPD) from the 0.125° spatial resolution land air temperature (T_a) and dew point temperature (T_d) ERA-Interim dataset, which is a reanalysis product based on the Integrated Forecast System of the European Centre for Medium-Range Weather Forecasts (ECMWF-IFS). The calculation (Dee et al. 2011) follows:

$$VPD = SVP - AVP$$

$$AVP = 6.112 \times f_w \times exp\left(\frac{17.67 \times T_d}{T_d + 243.5}\right)$$

$$SVP = 6.112 \times f_w \times exp\left(\frac{17.67 \times T_a}{T_a + 243.5}\right)$$

where SVP and AVP are saturated vapor pressure and actual vapor pressure (hPa), respectively. T_a and T_d are the land air temperature (°C) and dew point temperature (°C), respectively.

$$f_w = 1 + 7 \times 10^{-4} + 3.46 \times 10^{-6} \times P_{mst}$$

$$P_{mst} = P_{msl} \times \left(\frac{(T_a + 273.16)}{(T_a + 273.16) + 0.0065 \times Z}\right)^{5.625}$$

where P_{mst} is the air pressure, P_{msl} is the air pressure at mean sea level (1013.25 hPa) and Z is the altitude.

(2) ERA5-Land 2m T_{air}

The ERA5-Land 2m air temperature data were supplied by the European Centre for Medium Range Weather Forecasts (ECMWF). ERA5-Land is a reanalysis dataset providing a consistent view of the evolution of land variables over several decades at an enhanced resolution compared to ERA5 (Zhao, Gao et al., 2020). This parameter is the temperature of air at 2m above the surface of land, sea or in-land waters. It is calculated by interpolating between the lowest model level and the Earth's surface, taking account of the atmospheric conditions. The unit is kelvin (K) (Muñoz-Sabater et al., 2021).

(3) BESS SW

The Breathing Earth System Simulator (BESS) is a simplified process-based model that couples atmosphere and canopy radiative transfers, canopy photosynthesis, transpiration, and energy balance. It couples an atmospheric radiative transfer model and artificial neural network with forcings from MODIS atmospheric products.

(4) RTSIF

RTSIF dataset is in good agreement with the original TROPOMI SIF, and its accuracy is further validated against tower-based SIF (Chen et al., 2022). The TROPOspheric Monitoring Instrument (TROPOMI) on the Copernicus Sentinel-5P mission enables significant improvements in providing high spatial and temporal resolution SIF observations, but the short temporal coverage of the data records has limited its applications in long-term studies (Veefkind et al., 2012). RTSIF uses machine learning to reconstruct TROPOMI SIF for 2001-2020 with a spatial resolution of 0.05° and a temporal resolution of 8 days. We resample temporal resolution as monthly.

(5) GOSIF-derived GPP

The GOSIF-derived GPP are generated based on various SIF-GPP relationships for the period from 2000 to 2022. At site-level, the universal and biome-specific SIF-GPP relationships are established based on SIF soundings from Orbiting Carbon Observatory-2 (OCO-2) and GPP data from 64 EC sites (Li and Xiao, 2019). And at grid cell level, a SIF-GPP relationship is established based on 0.05° GOSIF data and tower GPP. All these SIF-GPP relationships with different forms (universal and biome-specific, with and without intercept) at both site and grid cell levels performed well in estimating GPP globally.

(6) FLUXCOM GPP

The FLUXCOM GPP are estimated from 3 machine learning methods (RF, ANN, MARS) which were forced with CRUNCEPv6 meteorological data and mean seasonal cycles of several MODIS based variables to merge carbon flux measurements from FLUXNET eddy covariance towers with remote sensing and meteorological data (Jung et al., 2019). FLUXCOM GPP was well validated and was provided at 0.5° spatial resolutions and monthly intervals from 1980-2013 (Tramontana et al., 2016).

T_{air} and SW can be obtained directly from the relevant website. All of datasets used in this study are listed in Table S3. The air temperature (T_{air}) gridded files are available at website: https://rda.ucar.edu/datasets/ds314.3/. The ERA-Interim reanalysis datasets are available at website: https://www.ecmwf.int/en/forecasts/datasets/reanalysis-datasets/era-interim. (Dee et al., 2011). The Breathing Earth System Simulator (BESS) incoming shortwave solar radiation (SW) gridded files are available at website: http://environment.snu.ac.kr/bess_rad/. (Ryu et al. 2018). The reconstructed TROPOMI solar-induced fluorescence dataset (RTSIF) is available at website: https://doi.org/10.6084/m9.figshare.19336346.v2. (Chen et al., 2022). The MODIS Enhanced Vegetation Index (EVI) data are available at website: https://modis.gsfc.nasa.gov/data/dataprod/ mod13.php. The GOSIF-derived GPP datasets are available at website: http://data.globalecology.unh.edu/data/GOSIF-GPP_v2/. (Li and Xiao, 2019). The FLUXCOM GPP are available at website: https://www.bgc-jena.mpg.de/geodb/projects/Home.php. (Jung et al., 2019)

Supplementary Figures

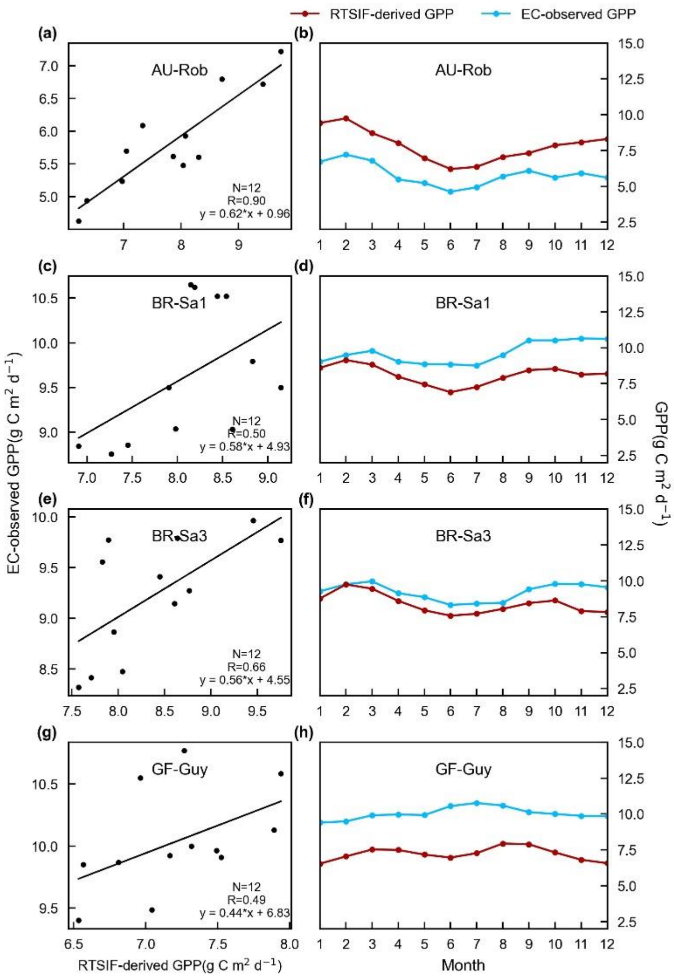

Figure S1. Comparisons between monthly RTSIF-derived GPP (red) and observed GPP at eddy covariance (EC) tower sites (blue). (a-b) Au-Rob, (c-d) BR-Sa1, (e-f) BR-Sa3, and (g-h) GF-Guy.

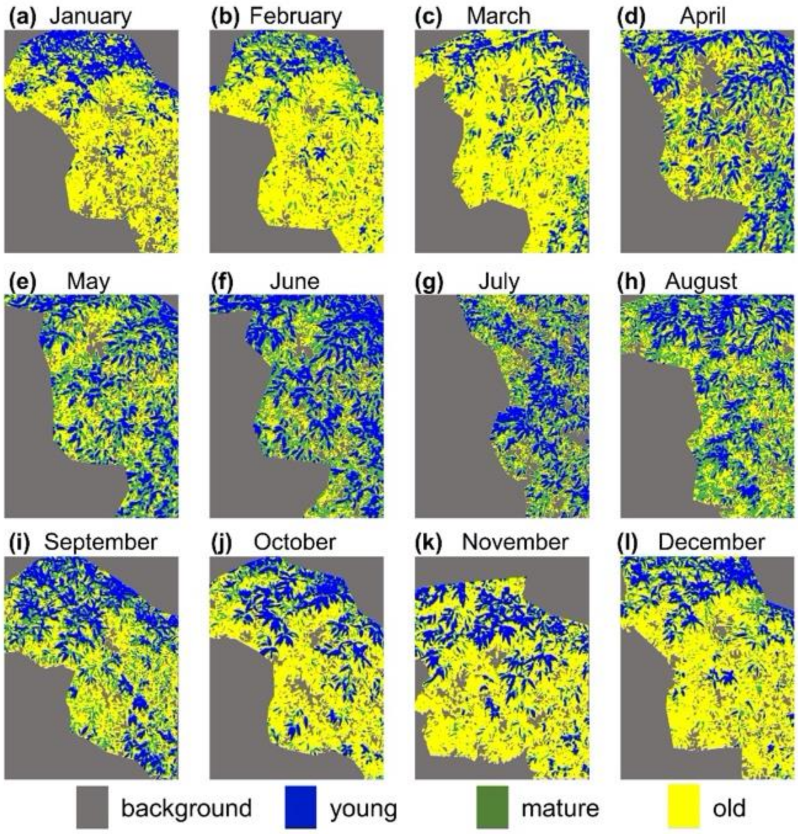

Figure S2. Classifications of canopy leaves into young, mature and old age cohorts in Dinghushan station. The boundaries of the imageries are those of the tree canopies that vary between months.

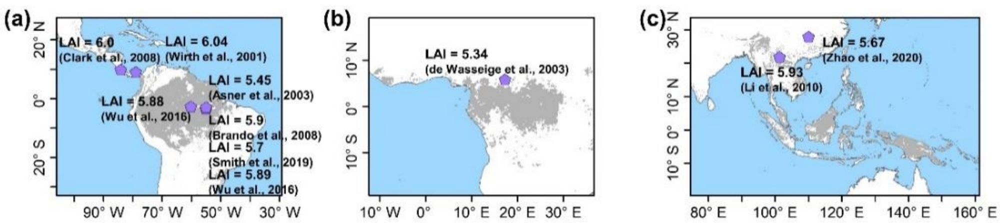

Figure S3. The distribution map of measured LAI sites from previously published literatures.

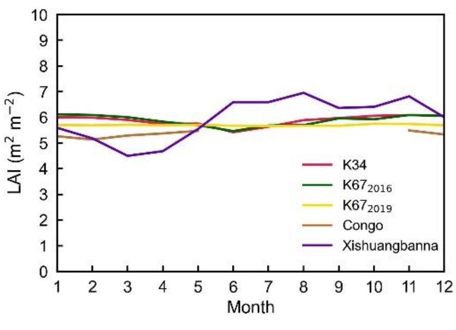

Figure S4. The seasonality of observed total LAI values from previously published literatures.

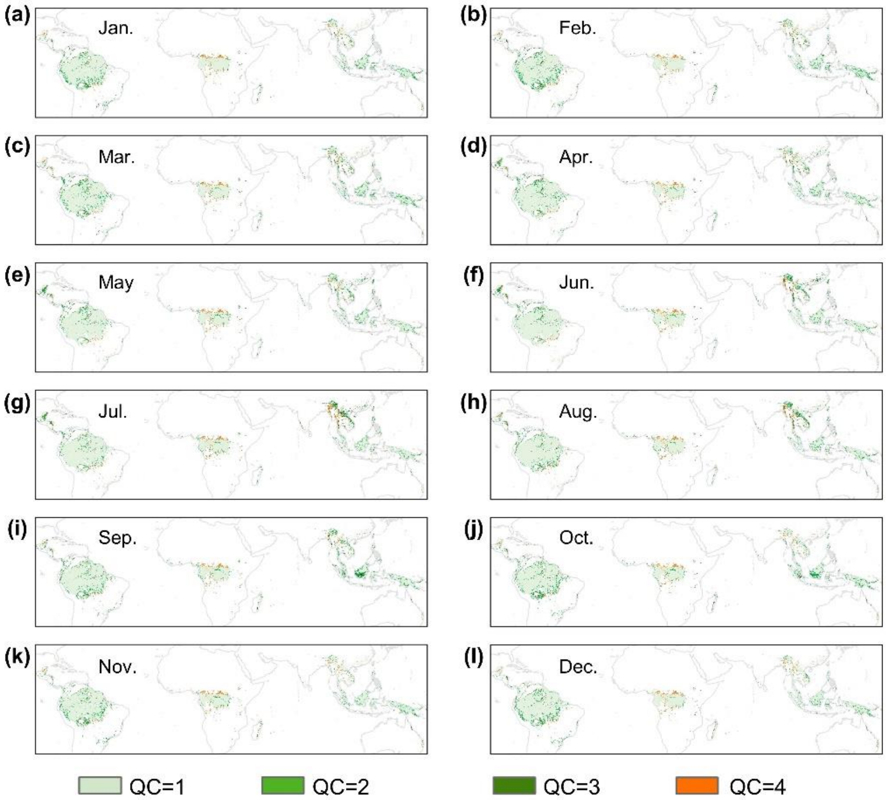

Figure S5. Spatial patterns of seasonal quality control (QC) datasets.

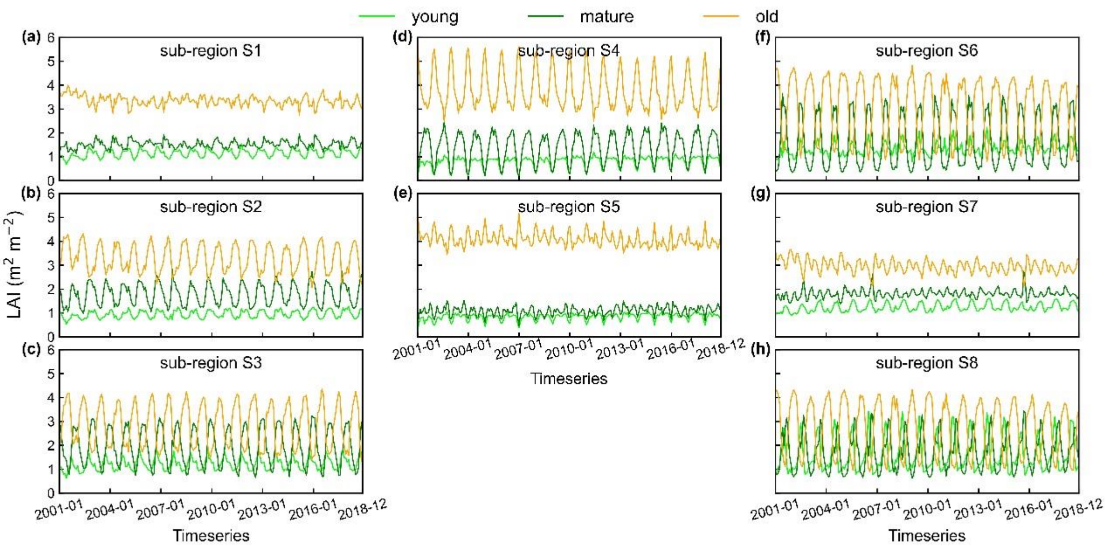

Figure S6. Timeseries of simulated LAI_{young}, LAI_{mature}, and LAI_{old} in 8 sub-regions classified by the K-means clustering analysis. Limegreen represents LAI_{young}; green represents LAI_{mature}; and orange represents LAI_{old}.

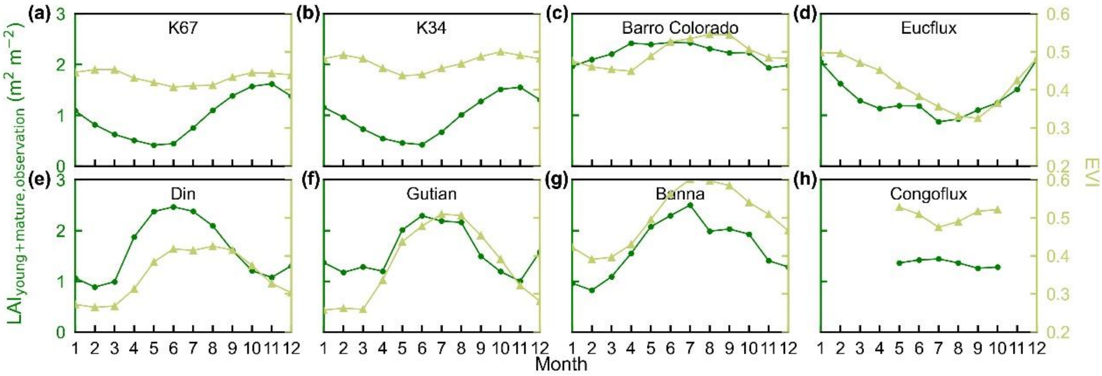

Figure S7. Comparison of the seasonality of $LAI_{young+mature}$ observations and MODIS Enhanced Vegetation Index (EVI) at eight camera-based observation sites. Green lines with circle markers present LAI observations; olive lines with triangle markers present EVI. (a) K67; (b) K34; (c) Barro Colorado; (d) EUCFLUX; (e) Din; (f) Gutian; (g) Banna; (h) CONGOFLUX

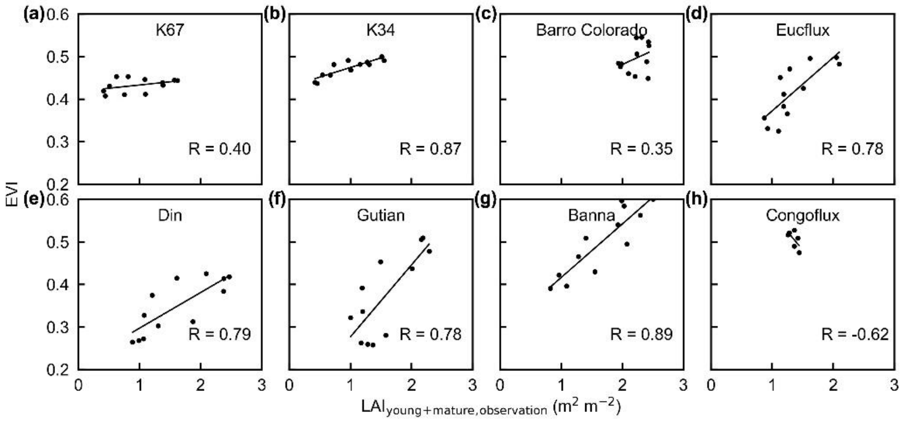

Figure S8. The scatterplots of observed $LAI_{young+mature}$ against EVI at 8 camera-based observation sites across study area.

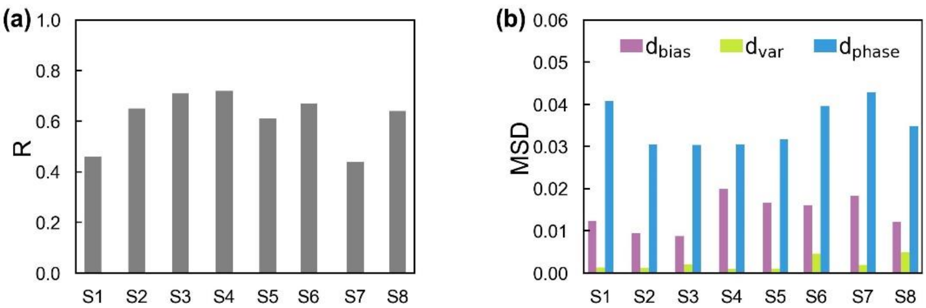

Figure S9. Statistics of the mean Pearson correlation coefficient (R) and mean squared deviation (MSD) between seasonality of simulated $LAI_{young+mature}$ and MODIS Enhanced Vegetation Index (EVI) in the 8 clustered sub-regions. (a) Mean of correlation coefficients in each sub-region; (b) mean of d_{bias}, d_{var} and d_{phase} in each sub-region.

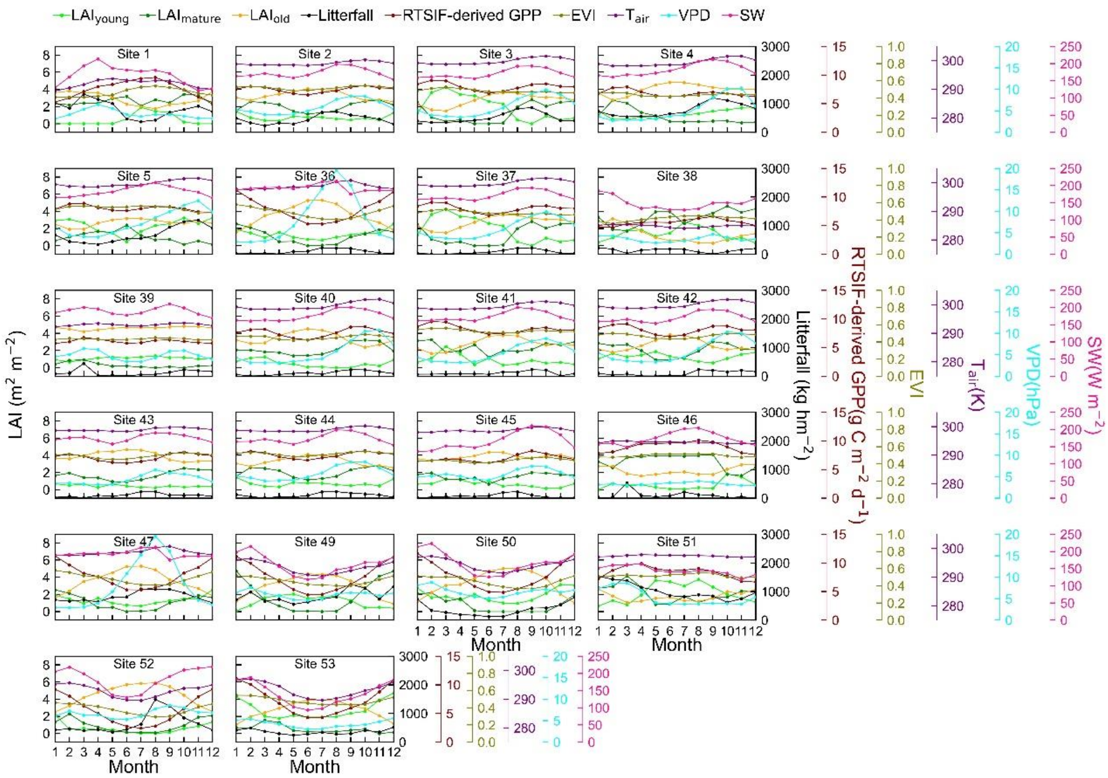

Figure S10. Seasonality of LAI_{young}, LAI_{mature}, LAI_{old}, litterfall, RTSIF-derived GPP, EVI, T_{air}, VPD and SW at 22 sites in south America.

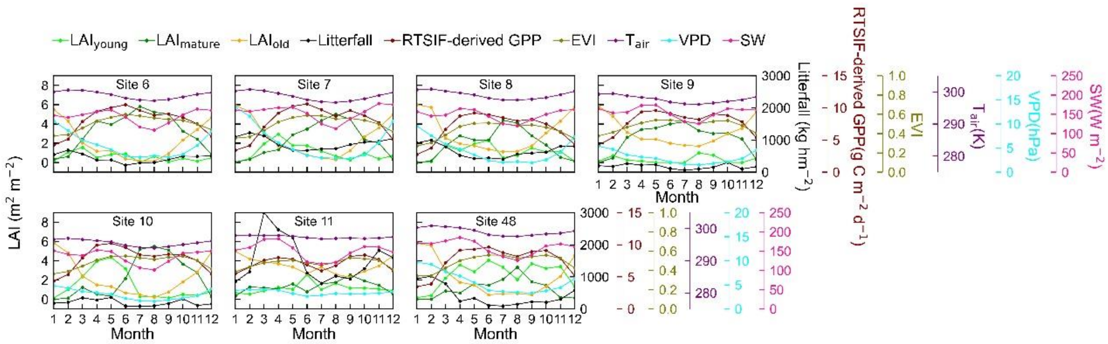

Figure S11. Seasonality of LAI_{young}, LAI_{mature}, LAI_{old}, litterfall, RTSIF-derived GPP, EVI, T_{air}, VPD and SW at 7 sites in Congo.

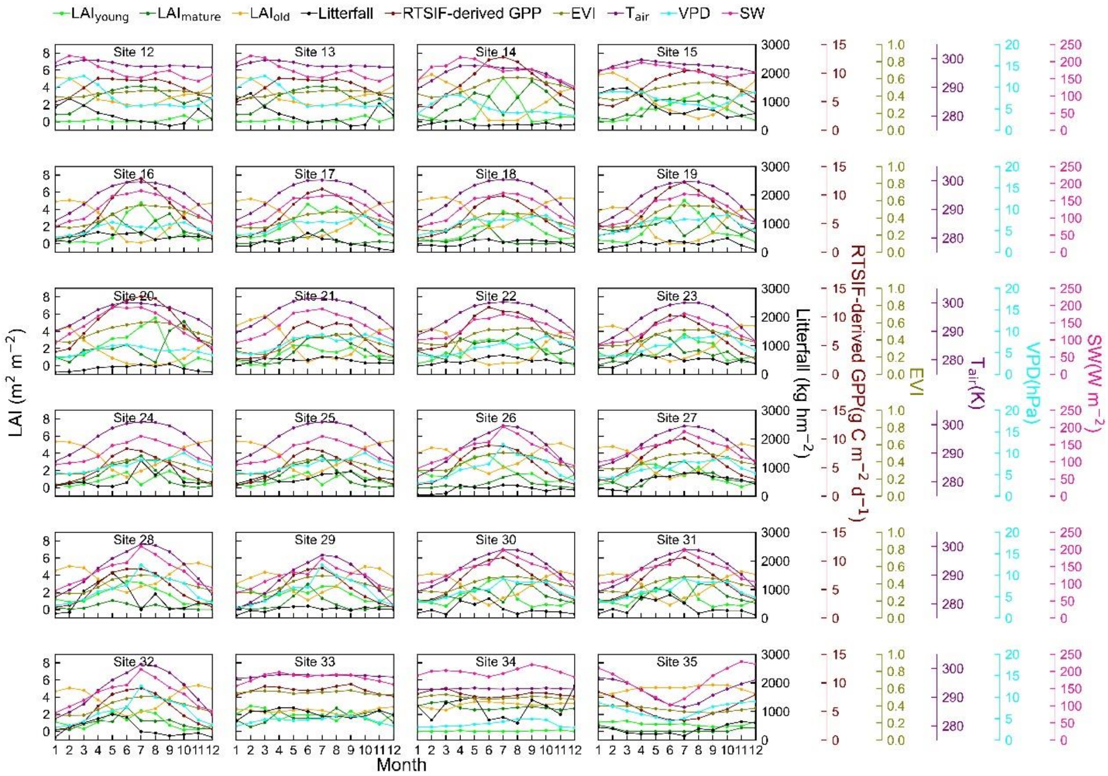

Figure S12. Seasonality of LAI$_{young}$, LAI$_{mature}$, LAI$_{old}$, litterfall, RTSIF-derived GPP, EVI, T$_{air}$, VPD and SW at 24 sites in tropical Asia.

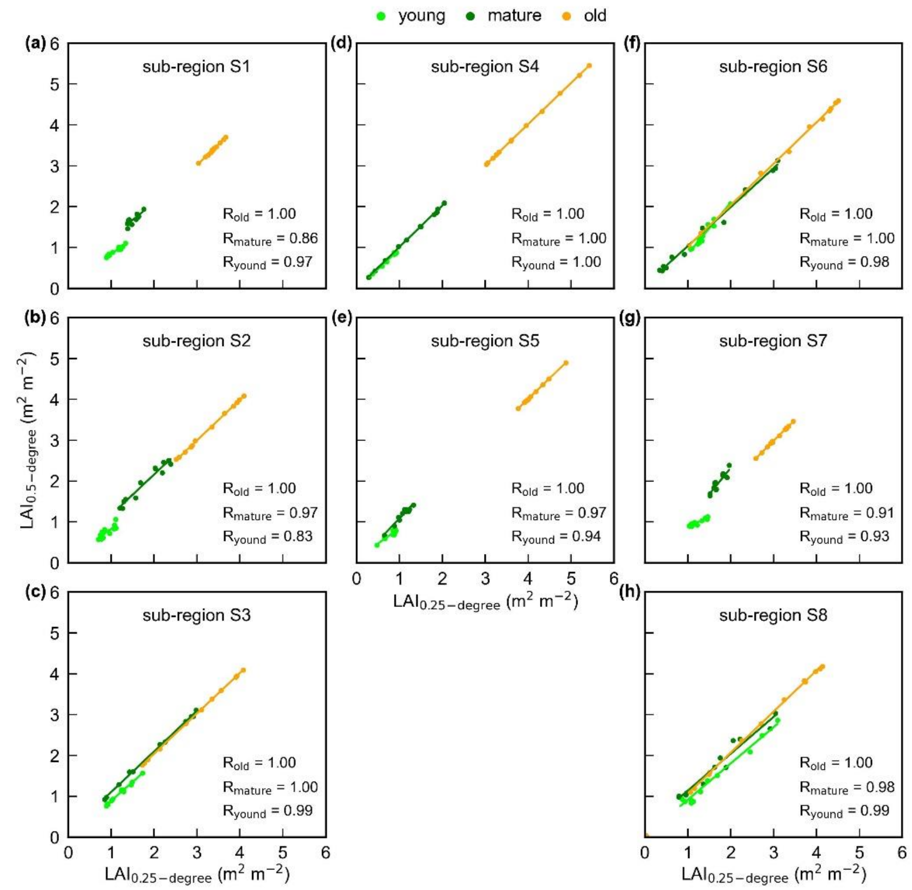

Figure S13. The scatterplot of 0.25-degree LAI_{young}, LAI_{mature}, LAI_{old} against 0.5-degree LAI cohort datasets in the 8 clustered regions.

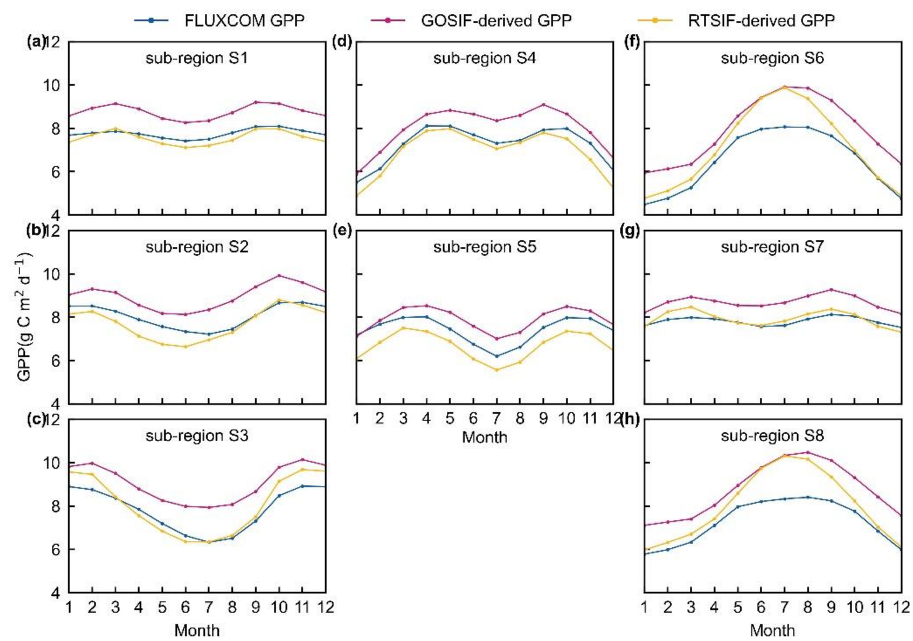

Figure S14. Seasonality of RTSIF-derived GPP (yellow lines), GOSIF-derived GPP (pink lines) and FLUXCOM GPP (blue lines) datasets in 8 sub-regions classified by the K-means clustering analysis. (a-c) South America; (d-e) Congo; (f-h) tropical Asia.

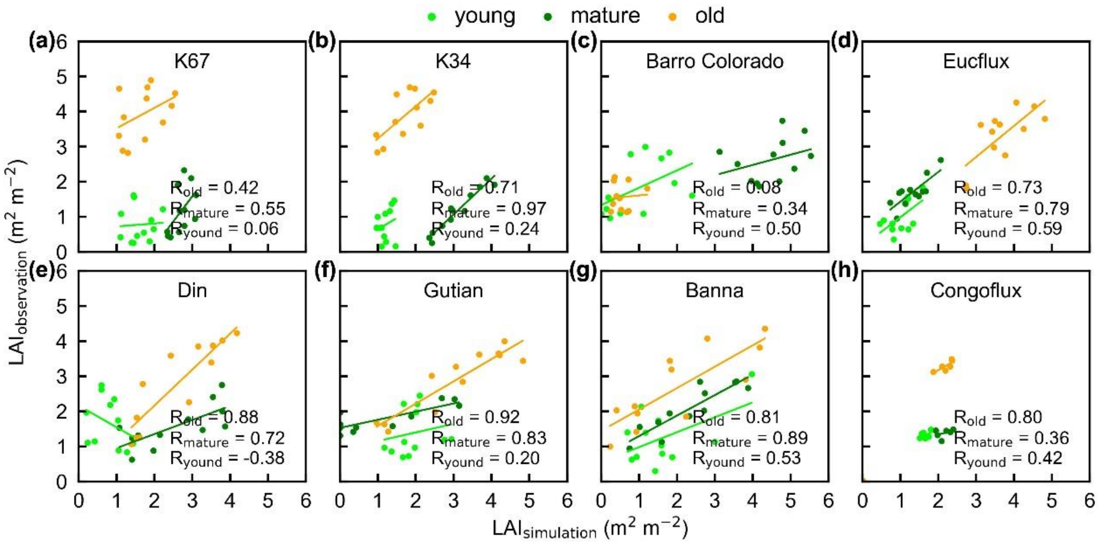

Figure S15. The scatterplots of simulated LAIs generated from GOSIF-derived GPP against observed LAIs at 8 camera-based observation sites across study area.

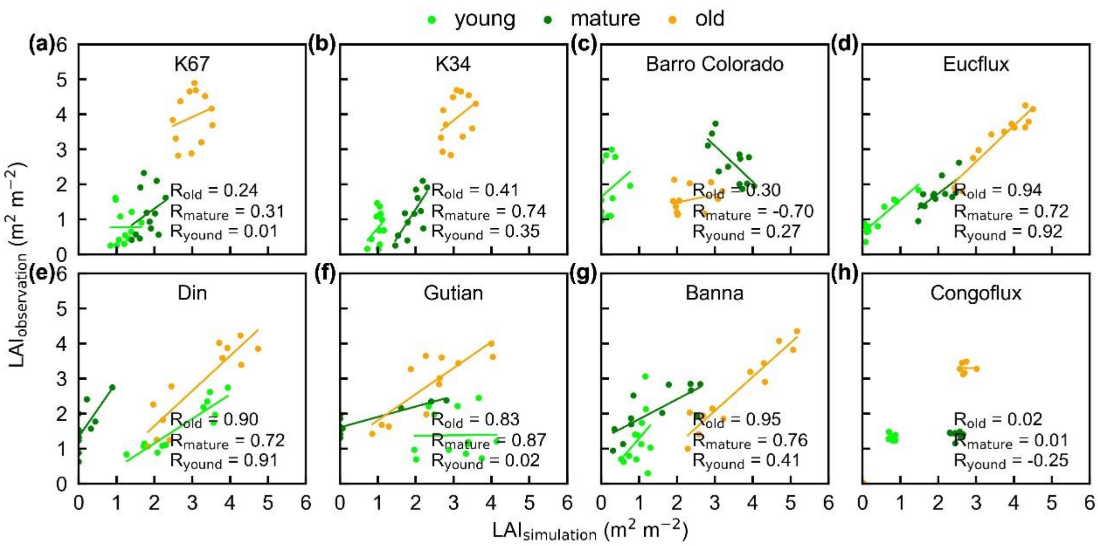

Figure S16. The scatterplots of simulated LAIs generated from FLUXCOM GPP against observed LAIs at 8 camera-based observation sites across study area.

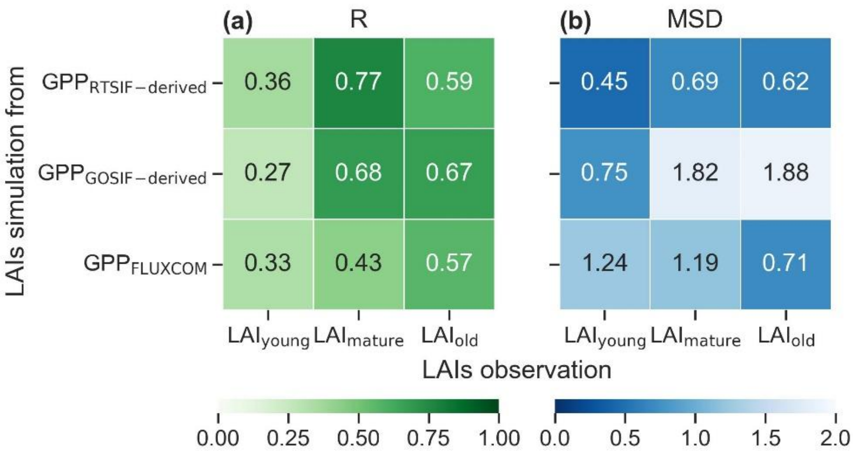

Figure S17. Comparison of RTSIF-derived GPP (upper panels), GOSIF-derived GPP (middle panels) and FLUXCOM GPP (bottom panels) datasets at 8 observation sites. (a) The correlation coefficients (R); (b) mean squared deviation (MSD).

Supplementary Tables

Table S1 Information of eight sites with observations of LAI cohorts

Site ID	Site Name	Latitude	Longitude
K67	Santarem-Km67-Primary Forest Ecosystem Research Station	-2.86	-54.96
K34	Manaus-K34 Forest Ecosystem Research Station	-2.61	-60.21
Barro Colorado	Smithsonian Tropical Research Institute, Barro Colorado Island, Panama	9.15	-79.85
Eucflux	Eucalyptus Plantation, Sao Paulo state, Brazil	-22.97	-48.73
Congoflux	Tropical Forest, DR Congo	0.81	24.50
Din	Dinghushan Forest Ecosystem Research Station	23.17	112.54
Gutian	Gutianshan Natural Reserve	29.23	118.40
Banna	Xishuangbanna Tropical Rainforest	21.92	101.27

Table S2 Information of four sites with observations of eddy covariance data

Site ID	Site Name	Latitude	Longitude
AU-Rob	Robson Creek, Queensland, Australia Forest Ecosystem Research Station	-17.12	145.63
BR-Sa1	Santarem-Km67-Primary Forest Ecosystem Research Station	-2.86	-54.96
BR-Sa3	Santarem-Km83-Logged Forest Ecosystem Research Station	-3.02	-54.97
GF-Guy	Guyaflux (French Guiana) Forest Ecosystem Research Station	5.28	-52.92

Table S3 Inputting gridded datasets to calculate the net rate of CO_2 assimilation (An) in Figure 2.

Name abbr.	Datasets Name	Source	Spatial-resolution	Time-resolution	During
T_{air}	temperature	ERA5-Land	0.1deg	monthly	195001-202112
VPD	vapor pressure deficit	ERA Interim	0.125deg	monthly	198201-201812
SW	downward short wave radiation	BESS	0.05deg	daily	200101-201912
RTSIF	sun-induced chlorophyll fluorescence	TROPOMI-SIF	0.05deg	8days	200101-201812
GOSIF GPP	gross primary production derived from OCO-2 Solar-induced chlorophyll fluorescence (GOSIF)	OCO-2 SIF	0.05deg	monthly	200001-202212
FLUXCOM GPP	gross primary production based on eddy covariance flux tower measurements	FLUXCOM	0.5deg	monthly	198001-201312

Table S4 -part1 Equations for calculating An, W_c, W_j and W_p and intermediate variables in Figure 2.

Equations	Notes	Ref.
$A_n = \min\left\{w_c, w_j, w_p\right\} - R_{dark}$	Net carbon assimilation rate (A_n, μmol/m^2/s).	Farquhar et al., 1980; Bernacchi et al., 2013
$w_c = V_{c\max} \times \frac{c_i - \Gamma^*}{c_i + K_C \times (1 + \frac{O}{K_O})}$	Rubisco-limited photosynthetic rate (w_c, μmol/m^2/s)	Farquhar et al., 1980
$w_j = J \times \frac{c_i - \Gamma^*}{4 \times (c_i + 2 \times \Gamma^*)}$	Electron-transport limited rate of photosynthetic rate (w_j, μmol/m^2/s)	Farquhar et al., 1980
$J = \frac{J_e + J_{\max} - \sqrt{(J_e + J_{\max})^2 - 4 \times \Theta \times J_e \times J_{\max}}}{2 \times \Theta}$	The rate of electrons through the thylakoid membrane (μmol/m^2/s)	Farquhar et al., 1980; Bernacchi et al., 2013
$J_e = PAR_{total} \times \alpha \times \beta \times \Phi_{PSII}$	The rate of whole electron transport provided by light (μmol/m^2/s).	Bernacchi et al., 2013
$w_p = 0.5 \times V_{c\max}$	Triose phosphate export limited rate of photosynthesis (μmol/m^2/s)	Ryu et al., 2011
$Para = Para_{25} \times \exp(\frac{(T_K - 298.15) \times \Delta H_{para}}{R \times T_K \times 298.15})$	Temperature dependence function for various parameters including K_C, K_O, Γ^*, R_{dark} and V_{cmax}. T_K denotes leaf temperature in Kelvin. Reference temperature is 25 °C.	Bernacchi et al., 2013
$J_{\max} = J_{\max,25} \times \exp((\frac{25 - T_{opt}}{\Omega_T})^2 - (\frac{T_K - 273.15 - T_{opt}}{\Omega_T})^2)$	Temperature dependence function for maximum electron transport rate (J_{max}). T_{opt} is the optimal temperature for $J_{max.}$	Bernacchi et al., 2013; June et al., 2004
$g_s = 1.6 \times (1 + \frac{g_1}{\sqrt{VPD}}) \times \frac{A_n}{c_a}$ $A_n = g_s \times (c_a - c_i)$ $\Rightarrow c_i = c_a \times (1 - \frac{1}{1.6 \times (1 + \frac{g_1}{\sqrt{VPD}})})$	Use optimal stomatal model to estimate internal CO_2 concentration (c_i) from atmospheric CO_2 concentration (c_a) and vapor pressure deficit (VPD)	Lin et al., 2015; Medlyn et al., 2011

Table S4 -part2 Equations for calculating An, W_c, W_j and W_p and intermediate variables in Figure 2.

Symbol/Equations	Notes	Ref.
$c_a = 380$	Atmospheric CO_2 concentration (ppm)	
$g_1 = 3.77$	Coefficient in stomatal conductance scheme	Lin et al., 2015
$J_{max,25} = 1.67 \times V_{c\max,25}$	Maximum electron transport rate (μmol/m^2/s) at 25 °C	Medlyn et al., 2002
$O = 210$	Atmospheric O_2 concentration (pp thousand)	
$R = 8.314$	Universal gas constant (J/K/mol)	
$T_{opt} = 35$	Optimal temperature for J_{max} (°C)	Lloyd and Farquhar, 2008
$K_{C,25} = 404.9$ $\Delta H_{K_C} = 79.43$	Michaelis-Menton constant for carboxylase (μmol/mol) at 25 °C and activation energy for temperature dependence (kJ/mol)	Bernacchi et al., 2001
$K_{O,25} = 278.4$ $\Delta H_{K_O} = 36.38$	Michaelis-Menton constant for oxygenase (mmol/mol) at 25 °C and activation energy for temperature dependence (kJ/mol)	Bernacchi et al., 2001
$R_{dark,25} = 0.015 \times V_{c\max,25}$ $\Delta H_{R_{dark}} = 46.39$	Leaf dark respiration (μmol/m^2/s) at 25 °C and activation energy for temperature dependence (kJ/mol)	Bernacchi et al., 2001
$V_{c\max,25}$ $\Delta H_{V_{c\max}} = 65.33$	Maximum carboxylation rate (μmol/m^2/s) at 25 °C is acquired from observations. Its activation energy for temperature dependence (kJ/mol) is listed	Bernacchi et al., 2001
$\Gamma^*_{25} = 42.75$ $\Delta H_{\Gamma^*} = 38.83$	CO_2 compensation point (μmol/mol) at 25 °C and activation energy for temperature dependence (kJ/mol)	Bernacchi et al., 2001
$\alpha = 0.85$	Leaf absorbance fraction of photosynthetically active radiation (PAR)	Farquhar et al., 1980; Bernacchi et al., 2013
$\beta = 0.5$	Fraction of PAR that reaches PSII system	Farquhar et al., 1980; Bernacchi et al., 2013
$\Phi_{PSII} = 0.85$	Maximum quantum efficiency of PSII photochemistry.	Bernacchi et al., 2003; Evans, 1989; von Caemmerer et al., 2000
$\Theta = 0.7$	Convexity of light-response curve.	Bernacchi et al., 2003; Evans, 1989; Ögren and Evans, 1993
$\Omega_T = 11.6 + 0.18 \times T_{opt}$	Coefficient for the temperature function of J_{max}. T_{opt} is optimal temperature for J_{max} (°C)	Bernacchi et al., 2003

Table S4 -part3 Equations for calculating An, W_c, W_j and W_p and intermediate variables in Figure 2.

Equations to calculate radiative transfer within canopy with a total leaf area index as LAI_{total}.

Equations	Notes	Ref.
$PAR_{total} = (1-\rho_{cb}) \times PAR_{b,0} \times \left(1-exp(-k_b' \times CI \times LAI_{total})\right) + (1-\rho_{cd}) \times PAR_{d,0} \times \left(1-exp(-k_d' \times CI \times LAI_{total})\right)$	Total PAR absorbed by canopy (μmol/m²/s)	He et al., 2012; Ryu et al., 2011; De Pury and Farquhar, 1997
$k_b' = \frac{0.46}{\cos(SZA)}$	Extinction coefficient for beam and scattered beam PAR	De Pury and Farquhar, 1997
$k_d' = 0.719$	Extinction coefficient for diffuse and scattered diffuse PAR	De Pury and Farquhar, 1997
$\rho_{cb} = 0.029$	Canopy reflection coefficient for beam PAR	De Pury and Farquhar, 1997
$\rho_{cd} = 0.036$	Canopy reflection coefficient for diffuse PAR	De Pury and Farquhar, 1997
$CI = 0.63$	Leaf clumping index	He et al., 2012; Ryu et al., 2011

Table S4 -part4 Equations for calculating An, W_c, W_j and W_p and intermediate variables in Figure 2.

Equations to calculate incoming photosynthetically active radiation in beam ($PAR_{b,0}$) and in diffuse ($PAR_{d,0}$) over canopy. R_{short} denotes total short-wave radiations from BESS SW. P denotes observed air pressure and P_0 denotes standard air pressure.

Equations	Notes	Ref.
$PAR_{b,0} = R_{short} \times f_{PAR} \times f_{PAR,b}$ $PAR_{d,0} = R_{short} \times f_{PAR} \times (1 - f_{PAR,b})$	The canopy top photosynthetically active radiation in beam ($PAR_{b,0}$) and diffuse ($PAR_{d,0}$) light	Weiss and Norman, 1985
$f_{PAR} = \frac{R_{b,vis} + R_{d,vis}}{R_{b,nir} + R_{d,nir} + R_{b,vis} + R_{d,vis}}$ $f_{PAR,b} = \frac{R_{b,vis}}{R_{b,vis} + R_{d,vis}} \times (1 - (\frac{0.9 - \frac{R_{short}}{R_{b,nir} + R_{d,nir} + R_{b,vis} + R_{d,vis}}}{0.7})^2)$	The fraction of total PAR over total incoming radiation (f_{PAR}) and the fraction of beam PAR over total PAR ($f_{PAR,b}$)	Weiss and Norman, 1985
$R_{b,vis} = \frac{600 \times e^{-0.185 \times \frac{P}{P_0} \times m}}{m}$	Expected beam visible radiation under clear sky (W/m^2)	Weiss and Norman, 1985
$R_{d,vis} = \frac{0.4 \times (600 - R_{b,vis} \times m)}{m}$	Expected diffuse visible radiation under clear sky (W/m^2)	Weiss and Norman, 1985
$R_{b,nir} = \frac{720 \times e^{-0.06 \times \frac{P}{P_0} \times m} - w}{m}$	Expected beam near-infrared radiation under clear sky (W/m^2)	Weiss and Norman, 1985
$R_{d,nir} = \frac{0.6 \times (720 - R_{b,nir} \times m - w)}{m}$	Expected diffuse near-infrared radiation under clear sky (W/m^2)	Weiss and Norman, 1985
$w = 1320 \times 10^{-1.195 + 0.4459 \times \log_{10} m - 0.0345 \times (\log_{10} m)^2}$	Expected water absorbance of near-infrared radiation in the atmosphere (W/m^2)	Weiss and Norman, 1985
$m = \cos(SZA)^{-1}$	Parameter calculated from solar zenith angle (SZA)	Weiss and Norman, 1985

Table S5. Information of total LAI mean values from previously published literatures.

NO.	LAI mean	Sites	Methods	Ref.
1	6.0	ORCHIDEE TrBE module	Module	De Weirdt et al., 2012
2	5.88	K34	observation	Wu et al., 2016
3	5.45	Tapajo´s National Forest	observation	Asner et al., 2003
4	6.04	Barro Colorado Island	observation	Wirth et al., 2001
5	6.0	Costa Rican Forest	observation	Clark et al., 2008;
6	5.89	K67	observation	Wu et al., 2016
7	5.9	Tapajo´s National Forest	observation	Brando et al., 2008
8	5.7	K67	observation	Smith et al., 2019
9	5.34	Congo	observation	de Wasseige et al., 2003
10	5.93	Xishuangbanna	observation	Li et al., 2010
11	5.67	Dinghushan	observation	Zhao, Chen et al., 2020

Table S6. Information of 53 sites with ground-based observations of seasonal litterfall data.

Site	Latitude	Longitude	Reference
1	15.50	-90.45	Kunkel-Westphal and Kunkel, 1979
2	-2.61	-60.21	Pastorello et al., 2020
3	-2.85	-54.95	Pastorello et al., 2020
4	-0.45	-51.70	Barlow et al., 2007
5	-1.73	-47.15	Dantas and Phillipson, 1989
6	6.85	4.35	Hopkins, 1966
7	7.48	4.57	Odiwe and Muoghalu, 2003
8	5.70	6.20	Ndakara, 2011
9	4.57	9.45	Songwe and Fasehun, 1995
10	4.37	9.27	Songwe and Fasehun, 1995
11	0.51	12.80	Midoko Iponga et al., 2019
12	8.48	77.28	Sundarapandian and Swamy, 1999
13	8.47	77.36	Sundarapandian and Swamy, 1999
14	21.93	101.27	CERN
15	14.50	101.92	Yamashita et al., 2010
16	22.13	106.82	Lu et al., 2008
17	21.93	108.35	Wu, 1991
18	22.97	108.35	Rong, 2009
19	23.01	108.59	Zeng, 2011
20	19.12	109.95	Wang, 2007
21	21.08	110.17	Ren et al., 1998
22	21.85	111.02	Ren et al., 1998
23	23.47	111.87	Chen and Wang, 1992
24	22.68	112.90	Zou et al., 2006
25	22.68	112.90	CERN
26	26.10	117.20	Wu, 2006
27	24.33	117.43	Pan et al., 2010
28	26.19	117.43	Yang et al., 2003
29	27.70	117.68	Lin et al., 1999
30	24.77	117.86	Liu et al., 2009

31	24.77	117.86	Tang, 2010
32	26.47	117.95	Zheng et al., 2011
33	4.97	117.80	Burghouts et al., 1992
34	-1.52	120.03	Triadiati et al., 2011
35	-27.33	152.75	Hegarty, 1991
36	-11.42	-55.33	Zhang et al., 2014
37	-2.85	-54.95	Rice et al., 2004
38	4.79	-74.20	Zhang et al., 2014
39	5.45	-61.88	Zhang et al., 2014
40	-1.00	-52.00	Zhang et al., 2014
41	-3.01	-54.97	Melton et al., 2014
42	-2.00	-54.00	Zhang et al., 2014
43	-4.33	-62.47	Zhang et al., 2014
44	-2.57	-60.12	Wu et al., 2016
45	5.27	-52.92	De Weirdt et al., 2012
46	7.20	-75.34	Zhang et al., 2014
47	-11.42	-55.33	Zhang et al., 2014
48	6.22	-5.03	Zhang et al., 2014
49	-23.14	-44.18	Silva-Filho et al., 2006
50	-21.02	-40.92	Jackson, 1978
51	9.38	-79.96	Unpublished data, S. J. Wright
52	-23.18	-46.87	Morellato, 1992
53	-25.18	-48.30	Scheer et al., 2009

Table S7. Information of data quality control (QC) for the Lad-LAI product

QC class	QC value	RSS	RMSE (m^2 m^{-2})
Best	1	0-1	0-1
Good	2	1-4	1-2
Acceptable	3	4-9	2-3
Cautious use	4	>9	>3

References:

Asner, G.P., Scurlock, J.M.O. and A. Hicke, J.: Global synthesis of leaf area index observations: implications for ecological and remote sensing studies, Global Ecol. Biogeogr., 12, 191-205, 10.1046/j.1466-822X.2003.00026.x, 2003.

Barlow, J., Gardner, T. A., Ferreira, L. V., and Peres, C. A.: Litter fall and decomposition in primary, secondary and plantation forests in the Brazilian Amazon, Forest Ecol. Manag., 247, 91-97, 10.1016/j.foreco.2007.04.017, 2007.

Bernacchi, C. J., Singsaas, E. L., Pimentel, C., Portis Jr, A. R., and Long, S. P.: Improved temperature response functions for models of Rubisco-limited photosynthesis, Plant, Cell Environ., 24, 253-259, 10.1111/j.1365-3040.2001.00668.x, 2001.

Bernacchi, C. J., Pimentel, C., and Long, S. P.: In vivo temperature response functions of parameters required to model RuBP-limited photosynthesis, Plant, Cell Environ., 26, 1419-1430, 10.1046/j.0016-8025.2003.01050.x, 2003.

Bernacchi, C. J., Bagley, J. E., Serbin, S. P., Ruiz-Vera, U. M., Rosenthal, D. M., and Vanloocke, A.: Modelling C_3 photosynthesis from the chloroplast to the ecosystem, Plant, Cell Environ., 36, 1641-1657, 10.1111/pce.12118, 2013.

Brando, P. M., Nepstad, D. C., Davidson, E. A., Trumbore, S. E., Ray, D. and Camargo, P.: Drought effects on litterfall, wood production and belowground carbon cycling in an Amazon forest: Results of a throughfall reduction experiment, Philos. T. R. Soc. B., 363, 1839-1848, 10.1098/rstb.2007.0031, 2008.

Burghouts, T., Ernsting, G., Korthals, G., and Vries, T. D.: Litterfall, leaf litter decomposition and litter invertebrates in primary and selectively logged dipterocarp forest in Sabah, Malaysia, Philos. T. R. Soc. B., 335, 407-416, 10.1098/rstb.1992.0032, 1992.

Chinese Ecosystem Research Network (CERN): http://www.cnern.org.cn., last access: 13 November 2022.

Chen, X., Huang, Y., Nie, C., Zhang, S., Wang, G., Chen, S., and Chen, Z.: A long-term reconstructed TROPOMI solar-induced fluorescence dataset using machine learning algorithms, Sci. Data, 9, 427, 10.1038/s41597-022-01520-1, 2022.

Chen, Z. H., Zhang, H. T., and Wang, B. S.: Studies on biomass and production of the lower subtropical evergreen broad-leaved forest in Heishiding Natural Reserve, VII. Litterfall, litter standing crop and litter decomposition rate, Journal of Tropical and Subtropical Botany, 107-114, http://europepmc.org/abstract/CBA/539457, 1992.

Clark, D.B., Olivas, P.C., Oberbauer, S.F., Clark, D.A. and Ryan, M.G.: First direct landscape-scale measurement of tropical rain forest Leaf Area Index, a key driver of global primary productivity, Ecol. Lett., 11, 163-172, 10.1111/j.1461-0248.2007.01134.x, 2008.

Dantas, M. and Phillipson, J.: Litterfall and litter nutrient content in primary and secondary Amazonian ‘terra firme’ rain forest, J. Trop. Ecol., 5, 27-36, 10.1017/s0266467400003199, 1989.

De Pury, D. G. G. and Farquhar, G. D.: Simple scaling of photosynthesis from leaves to canopies without the errors of big-leaf models, Plant, Cell Environ., 20, 537-557, 10.1111/j.1365-3040.1997.00094.x, 1997.

de Wasseige, C., Bastin, D. and Defourny, P.: Seasonal variation of tropical forest LAI based on field measurements in Central African Republic, Agr. Forest Meteorol., 119, 181-194, 10.1016/S0168-1923(03)00138-2, 2003.

De Weirdt, M., Verbeeck, H., Maignan, F., Peylin, P., Poulter, B., Bonal, D., Ciais, P., and Steppe, K.: Seasonal leaf dynamics for tropical evergreen forests in a process-based global ecosystem model, Geosci. Model Dev., 5, 1091-1108, 10.5194/gmd-5-1091-2012, 2012.

Dee, D. P., Uppala, S. M., Simmons, A. J., Berrisford, P., Poli, P., Kobayashi, S., Andrae, U., Balmaseda, M. A., Balsamo, G., Bauer, P., Bechtold, P., Beljaars, A. C. M., van de Berg, L., Bidlot, J., Bormann, N., Delsol, C., Dragani, R., Fuentes, M., Geer, A. J., Haimberger, L., Healy, S. B., Hersbach, H., Hólm, E. V., Isaksen, L., Kållberg, P., Köhler, M., Matricardi, M., McNally, A. P., Monge-Sanz, B. M., Morcrette, J. J., Park, B. K., Peubey, C., de Rosnay, P., Tavolato, C., Thépaut, J. N., and Vitart, F.: The ERA-Interim reanalysis: configuration and performance of the data assimilation system, Q. J. Roy. Meteor. Soc., 137, 553-597, 10.1002/qj.828, 2011.

Evans, J. R.: Photosynthesis and Nitrogen Relationships in Leaves of C_3 Plants, Oecologia, 78, 9-19, jstor.org/stable/4218825, 1989.

Farquhar, G. D., von Caemmerer, S., and Berry, J. A.: A biochemical model of photosynthetic CO_2 assimilation in leaves of C_3 species, Planta, 149, 78-90, 10.1007/BF00386231, 1980.

He, L., Chen, J. M., Pisek, J., Schaaf, C. B., and Strahler, A. H.: Global clumping index map derived from the MODIS BRDF product, Remote Sens. Environ., 119, 118-130, 10.1016/j.rse.2011.12.008, 2012.

Hegarty, E. E.: Leaf litter production by lianes and trees in a sub-tropical Australian rain forest, J. Trop. Ecol., 7, 201-214, 10.1017/s0266467400005356, 1991.

Hopkins, B.: Vegetation of the Olokemeji Forest Reserve, Nigeria: IV. The litter and soil with special reference to their seasonal changes, J. Ecol., 54, 10.2307/2257811, 1966.

Jackson, F. J.: Seasonality of flowering and leaf-fall in a Brazilian subtropical lower montane moist forest, Biotropica, 10, 38-42, 10.2307/2388103, 1978.

June, T., Evans, J. R., and Farquhar, G. D.: A simple new equation for the reversible temperature dependence of photosynthetic electron transport: a study on soybean leaf, Funct. Plant Biol., 31, 275-283, 10.1071/FP03250, 2004.

Jung, M., Koirala, S., Weber, U., Ichii, K., Gans, F., Camps-Valls, G., Papale, D., Schwalm, C., Tramontana, G., and Reichstein, M.: The FLUXCOM ensemble of global land-atmosphere energy fluxes, Sci. Data, 6, 74. 10.1038/s41597-019-0076-8, 2019.

Kunkel-Westphal, I. and Kunkel, P.: Litterfall in a guatemalan primary forest, with details of leaf-shedding by some common tree species, J. Ecol., 67, 10.2307/2259119, 1979.

Li, X., and Xiao, J.: Mapping photosynthesis solely from solar-induced chlorophyll fluorescence: A global, fine-resolution dataset of gross primary production derived from OCO-2, Remote Sens., 11, 2563, 10.3390/rs11212563, 2019.

Li, Z., Zhang, Y., Wang, S., Yuan, G., Yang, Y. and Cao, M.: Evapotranspiration of a tropical rain forest in Xishuangbanna, southwest China, Hydrol. Process., 24, 2405-2416, 10.1002/hyp.7643, 2010.

Lin, Y.-S., Medlyn, B. E., Duursma, R. A., Prentice, I. C., Wang, H., Baig, S., Eamus, D., de Dios, Victor R., Mitchell, P., Ellsworth, D. S., de Beeck, M. O., Wallin, G., Uddling, J., Tarvainen, L., Linderson, M.-L., Cernusak, L. A., Nippert, J. B., Ocheltree, T. W., Tissue, D. T., Martin-StPaul, N. K., Rogers, A., Warren, J. M., De Angelis, P., Hikosaka, K., Han, Q., Onoda, Y., Gimeno, T. E., Barton, C. V. M., Bennie, J., Bonal, D., Bosc, A., Löw, M., Macinins-Ng, C., Rey, A., Rowland, L., Setterfield, S. A., Tausz-Posch, S., Zaragoza-Castells, J., Broadmeadow, M. S. J., Drake, J. E., Freeman, M., Ghannoum, O., Hutley, Lindsay B., Kelly, J. W., Kikuzawa, K., Kolari, P., Koyama, K., Limousin, J.-M., Meir, P., Lola da Costa, A. C., Mikkelsen, T. N., Salinas, N., Sun, W., and Wingate, L.: Optimal stomatal behaviour around the world, Nat. Clim. Change, 5, 459-464, 10.1038/nclimate2550, 2015.

Lin, Y., He, J., Yang, Z., Liu, C., Lin, P., and Li, Z.: Yield and dynamics of litter in Castanopsis chinensis community in Wuyi Mountains, Journal of Xiamen University (Natural Science), 128-134, 1999. (in Chinese)

Liu, W., Fan, H., Gao, C., Huang, R., and Su, B.: Litter mass and nutrient flux in Eucalyptus plantation in continuous age series, J. Ecol., 28, 1928-1934, 2009. (in Chinese)

Lloyd, J. and Farquhar, G. D.: Effects of rising temperatures and [CO2] on the physiology of tropical forest trees, Philos. T. R. Soc. B., 363, 1811-1817, 10.1098/rstb.2007.0032, 2008.

Lu, L., Jia, H., He, R., Li, J., and Tan, S.: A preliminary study on litter falls of six kinds of plantations in the tropical South Asia, Forestry Science Research, 21, 346-352, 2008. (in Chinese)

Medlyn, B. E., Duursma, R. A., Eamus, D., Ellsworth, D. S., Prentice, I. C., Barton, C. V. M., Crous, K. Y., De Angelis, P., Freeman, M., and Wingate, L.: Reconciling the optimal and empirical approaches to modelling stomatal conductance, Glob. Change Biol., 17, 2134-2144, 10.1111/j.1365-2486.2010.02375.x, 2011.

Medlyn, B. E., Dreyer, E., Ellsworth, D., Forstreuter, M., Harley, P. C., Kirschbaum, M. U. F., Le Roux, X., Montpied, P., Strassemeyer, J., Walcroft, A., Wang, K., and Loustau, D.: Temperature response of parameters of a biochemically based model of photosynthesis. II. A review of experimental data, Plant, Cell Environ., 25, 1167-1179, 10.1046/j.1365-3040.2002.00891.x, 2002.

Melton, J., Shrestha, R., and Arora, V.: The influence of soils on heterotrophic respiration exerts a strong control on net ecosystem productivity in seasonally dry Amazonian forests, Biogeosciences, 11, 1151-1168, 10.5194/bgd-11-12487-2014, 2014.

Midoko Iponga, D., Mpikou, R. G. J., Loumeto, J., and Picard, N.: The effect of different anthropogenic disturbances on litterfall of a dominant pioneer rain forest tree in Gabon, Afr. J. Ecol., 58, 281-290, 10.1111/aje.12696, 2019.

Morellato, C. P.: Nutrient cycling in two south-east brazilian forests. I litterfall and litter standing crop, J. Trop. Ecol., 8, 205-215, 10.1017/S0266467400006362, 1992.

Muñoz-Sabater, J., Dutra, E., Agustí-Panareda, A., Albergel, C., Arduini, G., Balsamo, G., Boussetta, S., Choulga, M., Harrigan, S., Hersbach, H., Martens, B., Miralles, D. G., Piles, M., Rodríguez-Fernández, N. J., Zsoter, E., Buontempo, C., and Thépaut, J.-N.: ERA5-Land: a state-of-the-art global reanalysis dataset for land applications, Earth. Syst. Sci. Data, 13, 4349-4383, 10.5194/essd-13-4349-2021, 2021.

Ndakara, O. E.: Litterfall and nutrient returns in isolated stands of persea gratissima (avocado pear) in the rainforest zone of southern Nigeria, Ethiopian Journal of Environmental Studies and Management, 4, 10.4314/ejesm.v4i3.6, 2011.

Odiwe, A. I. and Muoghalu, J. I.: Litterfall dynamics and forest floor litter as influenced by fire in a secondary lowland rain forest in Nigeria, Trop. Ecol., 44, 241-249, 2003.

Ögren E. and Evans J.R.: Photosynthetic light-response curves. I. The influence of CO_2 partial pressure and leaf inversion, Planta, 189, 180-190, 1993.

Pan, H., Huang, S., Hong, W., Zhao, K., and Zhang, Z.: Litter mass and carbon return dynamics of three species of Acacia plantation, Journal of Fujian Forestry University, 30, 104-108, 10.13324/j.cnki.jfcf.2010.02.013, 2010. (in Chinese)

Pastorello, G., Trotta, C., Canfora, E., Chu, H., Christianson, D., Cheah, Y. W., Poindexter, C., Chen, J., Elbashandy, A., Humphrey, M., Isaac, P., Polidori, D., Reichstein, M., Ribeca, A., van Ingen, C., Vuichard, N., Zhang, L., Amiro, B., Ammann, C., Arain, M. A., Ardo, J., Arkebauer, T., Arndt, S. K., Arriga, N., Aubinet, M., Aurela, M., Baldocchi, D., Barr, A., Beamesderfer, E., Marchesini, L. B., Bergeron, O., Beringer, J., Bernhofer, C., Berveiller, D., Billesbach, D., Black, T. A., Blanken, P. D., Bohrer, G., Boike, J., Bolstad, P. V., Bonal, D., Bonnefond, J. M., Bowling, D. R., Bracho, R., Brodeur, J., Brummer, C., Buchmann, N., Burban, B., Burns, S. P., Buysse, P., Cale, P., Cavagna, M., Cellier, P., Chen, S., Chini, I., Christensen, T. R., Cleverly, J., Collalti, A., Consalvo, C., Cook, B. D., Cook, D., Coursolle, C., Cremonese, E., Curtis, P. S., D'Andrea, E., da Rocha, H., Dai, X., Davis, K. J., Cinti, B., Grandcourt, A., Ligne, A., De Oliveira, R. C., Delpierre, N., Desai, A. R., Di Bella, C. M., Tommasi, P. D., Dolman, H., Domingo, F., Dong, G., Dore, S., Duce, P., Dufrene, E., Dunn, A., Dusek, J., Eamus, D., Eichelmann, U., ElKhidir, H. A. M., Eugster, W., Ewenz, C. M., Ewers, B., Famulari, D., Fares, S., Feigenwinter, I., Feitz, A., Fensholt, R., Filippa, G., Fischer, M., Frank, J., Galvagno, M., Gharun, M., Gianelle, D., Gielen, B., Gioli, B., Gitelson, A., Goded, I., Goeckede, M., Goldstein, A. H., Gough, C. M., Goulden, M. L., Graf, A., Griebel, A., Gruening, C., Grunwald, T., Hammerle, A., Han, S., Han, X., Hansen, B. U., Hanson, C., Hatakka, J., He, Y., Hehn, M., Heinesch, B., Hinko-Najera, N., Hortnagl, L., Hutley, L., Ibrom, A., Ikawa, H., Jackowicz-Korczynski, M., Janous, D., Jans, W., Jassal, R., Jiang, S., Kato, T., Khomik, M., Klatt, J., Knohl, A., Knox, S., Kobayashi, H., Koerber, G., Kolle, O., Kosugi, Y., Kotani, A., Kowalski, A., Kruijt, B., Kurbatova, J., Kutsch, W. L., Kwon, H., Launiainen, S., Laurila, T., Law, B., Leuning, R., Li, Y., Liddell, M., Limousin, J. M., Lion, M., Liska, A. J., Lohila, A., Lopez-Ballesteros, A., Lopez-Blanco, E., Loubet, B., Loustau, D., Lucas-Moffat, A., Luers, J., Ma, S., Macfarlane, C., Magliulo, V., Maier, R., Mammarella, I., Manca, G., Marcolla, B., Margolis, H. A., Marras, S., Massman, W., Mastepanov, M., Matamala, R., Matthes, J. H., Mazzenga, F., McCaughey, H., McHugh, I., McMillan, A. M. S., Merbold, L., Meyer, W., Meyers, T., Miller, S. D., Minerbi, S., Moderow, U., Monson, R. K., Montagnani, L., Moore, C. E., Moors, E., Moreaux, V., Moureaux, C., Munger, J. W., Nakai, T., Neirynck, J., Nesic, Z., Nicolini, G., Noormets, A., Northwood, M., Nosetto, M., Nouvellon, Y., Novick, K., Oechel, W., Olesen, J. E., Ourcival, J. M., Papuga, S. A., Parmentier, F. J., Paul-Limoges, E., Pavelka, M., Peichl, M., Pendall, E., Phillips, R. P., Pilegaard, K., Pirk, N., Posse, G., Powell, T., Prasse, H., Prober, S. M., Rambal, S., Rannik, U., Raz-Yaseef, N., Rebmann, C., Reed, D., Dios, V. R., Restrepo-Coupe, N., Reverter, B. R., Roland, M., Sabbatini, S., Sachs, T., Saleska, S. R., Sanchez-Canete, E. P., Sanchez-Mejia, Z. M., Schmid, H. P., Schmidt, M., Schneider, K., Schrader, F., Schroder, I., Scott, R. L., Sedlak, P., Serrano-Ortiz, P., Shao, C., Shi, P., Shironya, I., Siebicke, L., Sigut, L., Silberstein, R., Sirca, C., Spano, D., Steinbrecher, R., Stevens, R. M., Sturtevant, C., Suyker, A., Tagesson, T., Takanashi, S., Tang, Y., Tapper, N., Thom, J., Tomassucci, M., Tuovinen, J. P., Urbanski, S., Valentini, R., van der Molen, M., van Gorsel, E., van Huissteden, K., Varlagin, A., Verfaillie, J., Vesala, T., Vincke, C., Vitale, D., Vygodskaya, N., Walker, J. P., Walter-Shea, E., Wang, H., Weber, R., Westermann, S., Wille, C., Wofsy, S., Wohlfahrt, G., Wolf, S., Woodgate, W., Li, Y., Zampedri, R., Zhang, J., Zhou, G., Zona, D., Agarwal, D., Biraud, S., Torn, M., and Papale, D.: The FLUXNET2015 dataset and the ONEFlux processing pipeline for eddy covariance data, Sci. Data, 7, 225, 10.1038/s41597-020-0534-3, 2020.

Ren, H., Peng, S., Liu, H., Yu, Z., and Fang, D.: Study on litter and its ecological benefits of tropical artificial mixed forest in Xiaoliang, J. Appl. Ecol., 11-15, 1998.

Rong, Y.: Study on dynamics of litter production, quality and decomposition of Eucalyptus urophylla × Eucalyptus grandis and Acacia crassicarpa plantations, Guangxi Universit, 2009. (in Chinese)

Ryu, Y., Jiang, C., Kobayashi, H., and Detto, M.: MODIS-derived global land products of shortwave radiation and diffuse and total photosynthetically active radiation at 5 km resolution from 2000, Remote Sens. Environ., 204, 812-825, 10.1016/j.rse.2017.09.021, 2018.

Ryu, Y., Baldocchi, D. D., Kobayashi, H., van Ingen, C., Li, J., Black, T. A., Beringer, J., van Gorsel, E., Knohl, A., Law, B. E., and Roupsard, O.: Integration of MODIS land and atmosphere products with a coupled-process model to estimate gross primary productivity and evapotranspiration from 1 km to global scales, Global Biogeochem. Cy., 25, n/a-n/a, 10.1029/2011gb004053, 2011.

Scheer, B. M., Gatti, G., Wisniewski, C., Mocochinski, Y. A., Cavassani, T. A., Lorenzetto, A., and Putini, F.: Patterns of litter production in a secondary alluvial Atlantic Rain Forest in southern Brazil, Braz. J. Bot., 32, 805-817, 2009.

Sharma, E. and Ambasht, R. S.: Litterfall, Decomposition and Nutrient Release in an Age Sequence of Alnus Nepalensis Plantation Stands in the Eastern Himalaya, J. Ecol., 75, 10.2307/2260309, 1987.

Silva-Filho, V. E., Machado, W., Oliveira, R. R., Sella M. S., Lacerda, and D. L.:Mercury deposition through litterfall in an Atlantic Forest at Ilha Grande, Southeast Brazil, Chemosphere, 65, 2477-2484, 2006.

Smith, M. N., Stark, S. C., Taylor, T. C., Ferreira, M. L., de Oliveira, E., Restrepo-Coupe, N., Chen, S., Woodcock, T., dos Santos, D. B., Alves, L. F., Figueira, M., de Camargo, P. B., de Oliveira, R. C., Aragão, L. E. O. C., Falk, D. A., McMahon, S. M., Huxman, T. E. and Saleska, S. R.: Seasonal and drought-related changes in leaf area profiles depend on height and light environment in an Amazon forest. New Phytol., 222, 1284-1297, 10.1111/nph.15726, 2019.

Songwe, N. C., Okali, D. U. U., and Fasehun, F. E.: Litter decomposition and nutrient release in a tropical rainforest, Southern Bakundu Forest Reserve, Cameroon, J. Trop. Ecol., 11, 333-350, 10.1017/s0266467400008816, 1995.

Sundarapandian, S. M. and Swamy, P. S.: Litter production and leaf-litter decomposition of selected tree species in tropical forests at Kodayar in the Western Ghats, India, Forest Ecol. Manag., 123, 231-244, 10.1016/s0378-1127(99)00062-6, 1999.

Tang, J.: Dynamics of litter fall and nutrient return in Eucalyptus grandis plantation, Journal of Nanchang Institute of Technology, 29, 60-64, 2010. (in Chinese)

Tramontana, G., Jung, M., Schwalm, C. R., Ichii, K., Camps-Valls, G., R'aduly, B., Reichstein, M., Arain, M. A., Cescatti, A., Kiely, G., Merbold, L., Serrano-Ortiz, P., Sickert, S., Wolf, S., and Papale, D.: Predicting carbon dioxide and energy fluxes across global FLUXNET sites with regression algorithms, Biogeosciences, 13, 4291-4313, 2016.

Triadiati, Tjitrosemi, S., Guhardja, E., Sudarsono, Qayim, I., and Leuschner, C.: Litterfall production and leaf-litter decomposition at natural forest and cacao agroforestry in central Sulawesi, Indonesia, Asian Journal of Biological Sciences, 4, 221-234, 10.3923/ajbs.2011.221.234, 2011.

Veefkind, J. P., Aben, I., McMullan, K., Förster, H., de Vries, J., Otter, G., Claas, J., Eskes, H. J., de Haan, J. F., Kleipool, Q., van Weele, M., Hasekamp, O., Hoogeveen, R., Landgraf, J., Snel, R., Tol, P., Ingmann, P., Voors, R., Kruizinga, B., Vink, R., Visser, H., and Levelt, P. F.: TROPOMI on the ESA Sentinel-5 Precursor: A GMES mission for global observations of the atmospheric composition for climate, air quality and ozone layer applications, Remote Sens. Environ., 120, 70-83, 10.1016/j.rse.2011.09.027, 2012.

Wang, M., Liu, Q., and Gao, J.: Litter dynamics of four plant communities affected by typhoon in the central hilly area of Hainan Island, Journal of Hainan Normal University (Natural Science), 156-160, 2007. (in Chinese).

Weiss, A. and Norman, J. M.: Partitioning solar radiation into direct and diffuse, visible and near-infrared components, Agr. Forest Meteorol., 34, 205-213, 10.1016/0168-1923(85)90020-6, 1985.

Wirth, R., Weber, B., and Ryel, R. J.: Spatial and temporal variability of canopy structure in a tropical moist forest, Acta Oecol., 22(5-6), 2001.

Wu, J., Albert, L. P., Lopes, A. P., Restrepo-Coupe, N., Hayek, M., Wiedemann, K. T., Guan, K., Stark, S. C., Christoffersen, B., Prohaska, N., Tavares, J. V., Marostica, S., Kobayashi, H., Ferreira, M. L., Campos, K. S., da Silva, R., Brando, P. M., Dye, D. G., Huxman, T. E., Huete, A. R., Nelson, B. W., and Saleska, S. R.: Leaf development and demography explain photosynthetic seasonality in Amazon evergreen forests, Science, 351, 972-976, 10.1126/science.aad5068, 2016.

Wu, Y.: Study on Litter and Nutrient Cycling in Four Kinds of Evergreen Plantations, Guangxi Forestry Technology, 38-41+28, 10.19692/j.cnki.gfs.1991.01.007, 1991. (in Chinese)

Wu, Z.: Litter quantity, composition and dynamics of human-promoted evergreen broad-leaved secondary forest, Mountain Journal, 215-221, 2006. (in Chinese)

Yamashita, N., Ohta, S., Sase, H., Luangjame, J., Visaratana, T., Kievuttinon, B., Garivait, H., and Kanzaki, M.: Seasonal and spatial variation of nitrogen dynamics in the litter and surface soil layers on a tropical dry evergreen forest slope, Forest Ecol. Manag., 259, 1502-1512, 10.1016/j.foreco.2010.01.026, 2010.

Yang, Y., Lin, P., Guo, J., Lin, R., Chen, G., He, Z., and Xie, J.: Litter quantity, nutrient return and litter decomposition in natural forest and plantation of Castanopsis grizii, J. Ecol., 1278-1289, 2003.

Zeng, S.: Litter yield analysis of fast-growing tree species Eucalyptus and Acacia plantation, Jilin Agriculture, 231-232, 2011. (in Chinese)

Zhang, H., Yuan, W., Dong, W., and Liu, S.: Seasonal patterns of litterfall in forest ecosystem worldwide, Ecol. Complex., 20, 240-247, 2014.

Zhao, P., Gao, L., Wei, J., Ma, M., Deng, H., Gao, J., and Chen, X.: Evaluation of ERA-Interim Air Temperature Data over the Qilian Mountains of China, Adv. Meteorol., 7353482, 10.1155/2020/7353482, 2020

Zhao, Y., Chen, X., Smallman, T. L., Flack-Prain, S., Milodowski, D. T., and Williams, M.: Characterizing the Error and Bias of Remotely Sensed LAI Products: An Example for Tropical and Subtropical Evergreen Forests in South China, Remote Sens., 12, 3122, 10.3390/rs12193122, 2020.

Zheng, J., Yang, z., Ling, h., and Chen, G.: Yield and monthly dynamics of litter in Phoebe plantation, Journal of Fujian Normal University (Natural Science), 27, 88-92, 2011. (in Chinese)

Zou, B., Li, Z., Ding, Y., and Tan, W.: Litter dynamic characteristics of four plantation forests in South subtropical zone, Journal of Ecology, 715-721, 2006. (in Chinese)